www.czasopisma.pan.pl PAN POLSKA AKADEMIA NAUK www.journals.pan.pl

Arch. Metall. Mater., Vol. 61 (2016), No 2B, p. 1057–1062

DOI: 10.1515/amm-2016-0178

K. DYBOWSKI*, J. SAWICKI*#, P. KULA*, B. JANUSZEWICZ *, R. ATRASZKIEWICZ*, S. LIPA*

THE EFFECT OF THE QUENCHING METHOD ON THE DEFORMATIONS SIZE OF GEAR WHEELS AFTER VACUUM CARBURIZING

This paper presents a comparison of the deformations and residual stresses in gear wheels after vacuum carburizing process with quenching in high-pressure nitrogen and oil. The comparison was made on a medium-sized gear wheels, made of AMS6265 (AISI 9310) steel. This steel is applied in the aerospace industry for gears. The study has provided grounds for an assessment of the effect of the method of quenching on the size of deformations. Compared to oil quenching, high-pressure gas quenching following vacuum carburizing resulted in more uniform and smaller deformations.

Keywords: thermo-chemical treatment, vacuum carburizing, carburized layer, quenching, quenching deformations, low-pressure carburizing

1. Introduction

The two basic methods of thermo-chemical treatment of machine parts and elements are carburizing and nitriding. They are currently implemented in specialized furnaces or universal ones, making possible, depending on the type, the cooling of components (including quenching) in oil baths or in a stream of gas under high pressure – usually nitrogen [1-6]. Both carburizing and nitriding are currently realized in a controlled manner that allows, using computer-aided design processes, accurate control of the morphology of the surface layer [2,3,7,8]. Nitriding can be applied for various types of steel and cast irons and in case of gears of small module pitch. Carburizing finds a very wide application in case of gears and toothed elements [1,3,5,9]. Vacuum carburizing process is better than conventional carburizing due to its efficiency; it also has certain other advantages, such as: no internal oxidation, higher uniformity of the carburizing layers produced in the process, energy efficiency and environmental friendliness [1-6].

Thermal treatment following vacuum carburizing can be realized – as in traditional carburization – in quenching oil, or in high-pressure gas as a quenching medium. Gas cooling media, mainly nitrogen, helium, hydrogen or the mixtures thereof, are environmentally friendly, and ensure a clean, metallic surface of the treated elements. Thus treated items do not require any additional post-treatment processing. On the other hand, oil quenching necessitates washing quenched parts, usually in alkaline baths, followed by rinsing and drying. This requires neutralisation of wastewater and disposing of oil particles collected in separators. Moreover, oil quenching installations are much more complicated and they occupy more space in quenching tank [10-14].

The greatest drawback of gas cooling is its ability to absorb heat. The effectiveness of gas-cooling of the carburized charge strongly depends on the type of gas, its pressure and on the flow rate of gas which circulates around the items being cooled down. Helium and hydrogen have the greatest quenching capability among the gases used in the process. Despite the higher heat transfer coefficient, both gases are less likely to be applied as modern cooling media in thermal treatment. Helium – because of its high price, what requires costly and complicated recycling installations. Hydrogen – because of the high risk of explosions and logistic issues. Currently performed research aim to eliminate this issues by storing hydrogen in metal hydride beds [11,15].

Nowadays, the charge is usually cooled with nitrogen in the chambers of furnaces adapted to operation at pressures of up to 2.5 MPa. These are one- and two-chamber furnaces and modular lines. A characteristic feature of a one-chamber furnace is that the same chamber is used both for heating and cooling the furnace feed. The charge is cooled by gas circulating in an enclosed working space of the furnace, directed towards the charge by a system of nozzles. A two-chamber furnace has separated heating and cooling chamber in which the batch is quenched. The aim of the separation of cooling chamber is to ensure a greater intensity of quenching. In mass production, where treatment processes should be intensified because of the large number of items, modular lines are used, in which, one cooling chamber serves several vacuum-carburizing chambers. As with gas quenching, carburizing and oil-quenching furnaces

* LODZ UNIVERSITY OF TECHNOLOGY, INSTITUTE OF MATERIALS SCIENCE AND ENGINEERING,1/15 STEFANOWSKIEGO STR., 90-924 LODZ, POLAND

Corresponding author: jacek.sawicki@edu.p.lodz.pl

are two-chamber furnaces, additionally equipped with an oil bath in which items are quenched. While oil quenching has the disadvantages mentioned above, it has one advantage compared to gas quenching this is higher heat transfer coefficient, which enables the quenching of parts made of steel of lower hardenability; therefore, this cooling method is still applied in industry [10-14,16].

The aim of this study is to compare the deformations of medium-sized gear wheels made of AMS6265 (AISI 9310) steel, after vacuum carburizing process with high-pressure gas-quenched or oil-quenched, to identify the beneficial conditions of thermal treatment.

2. Material and methods

Gear wheels made of AMS6265 steel (chemical composition Tab. 1), of module m = 5 and the number of teeth = 30 were vacuum carburized (Fig. 1). Carburizing was done in a one-chamber furnace with high-pressure nitrogen cooling and in a two-chamber furnace with an oil bath – both devices manufactured by Seco/Warwick S.A. The dimensions of the furnace heating chamber: 400×400×600 mm. Each gear wheel was positioned vertically in the middle area of the furnace chamber on a special device, which guaranteed the well-defined and repeatable deployment during carburizing and cooling. The first two teeth of each wheel were marked permanently on their side surfaces to ensure the repeatable conditions of the experiment (as shown in Fig. 1). Gear wheels, before the carburizing process, were annealed in vacuum at 860°C for 3 hours. The carburizing atmosphere consisted of a mixture of acetylene – ethylene – hydrogen. Carburization was done in the FineCarb® technology [17]. The parameters of the carburized layer were designed: surface carbon concentration = 0.75%$_{wt.}$, effective case depth = 0.5 mm (for criterion = 0.4%$_{wt.}$C). In order to achieve the desired carbon concentration profile, the duration of the boost/diffusion process segments was selected based on the simulation made using the SimVaCPlus® program.

The vacuum carburizing process stages are described below:

- pumping up to pressure 10 Pa,
- soaking for 20 min. at 950°C,
- vacuum carburizing at 950°C, at pressure 300÷800 Pa, boost/diffusion time [min.]: 6:00/13:00, 4:00/34:30, 3:30/16:00,
- heating up to temperature 950°C with ramp 10°C/min.,
- precooling to temperature 860°C and soaking for 20 min.,
- gas quenching (nitrogen) to 50°C at a pressure of 1.4 MPa or oil quenching at a temperature of 50°C in an oil bath with stirring.

TABLE 1

Chemical composition AMS 6265 steel (%wt.)

C	Mn	Cr	Ni	Mo	Si
0,126	0,530	1,017	3,243	0,137	0,243

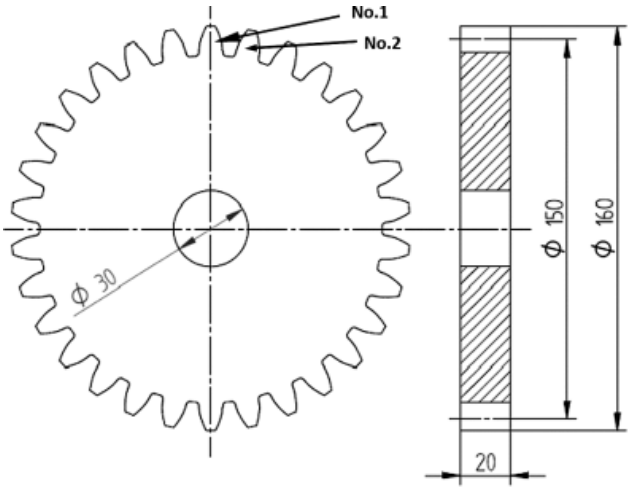

Fig. 1. Gearwheel used in researches, module = 5, number of teeth = 30

3. Results and discussion

The martensitic structure with retained austenite of similar concentrations was obtained in both cases (Fig. 2 and 3). The amount of retained austenite was 21±2% after gas quenching, and 19±3% after oil quenching. The content of retained austenite was determined by X-ray method with use of PROTO iXRD diffractometer. The surface layer carbon profiles obtained in the vacuum carburizing processes are shown in Fig. 4. The carbon concentration in a layer was measured with a glow discharge optical emission spectrometer – LECO GDS850A.

Retained austenite content was measured in compliance with ASTM E-975. Since steel contains crystalline phases such as ferrite or martensite and austenite, a unique X-ray diffraction pattern for each crystalline phase is produced when the steel sample is irradiated with X-radiation. For a randomly oriented sample, quantitative measurements of the relative volume fraction of ferrite and austenite can be made from X-ray diffraction patterns because the total integrated intensity of all diffraction peaks for each phase is proportional to the volume fraction of that phase.

For steel containing only ferrite (α) and austenite (γ) and no carbides, the integrated intensity from the (hkl) planes of the ferrite phase is expressed as.

$$I_{\alpha}^{hkl} = KR_{\alpha}^{hkl}V_{\alpha} / 2\mu$$

Where K is a constant which is dependent upon the selection of instrumentation geometry and radiation but independent of the nature of the sample. The parameter, R, is proportional to the theoretical integrated intensity. The parameter, R, depends upon interplanar spacing (hkl), the Bragg angle, θ, crystal structure, and composition of the phase being measured.

A similar equation applies to austenite. For any pair of austenite and ferrite (or martensite) hkl peaks:

$$\frac{I_{\alpha}^{hkl}}{I_{\gamma}^{hkl}} = \left(\frac{R_{\alpha}^{hkl}}{R_{\gamma}^{hkl}}\right) \times \left(\frac{V_{\alpha}}{V_{\gamma}}\right)$$

The volume fraction of austenite ($V\gamma$) for the ratio of measured integrated intensities of ferrite (or martensite) and austenite peak to R – value is

$$V_\gamma = \left[\frac{\frac{I_\gamma}{R_\gamma}}{\frac{I_\alpha}{R_\alpha}} + \frac{I_\gamma}{R_\gamma} \right]$$

To characterize the concentration of retained austenite using PROTOiXRD four diffraction peaks are collected by the instrument, two for the austenite , namely {200} and {220} and two for martensite, namely {200} and {211}. A comparison of the intensities of the 4 peaks yields the volume percent concentration of retained austenite in the sample.

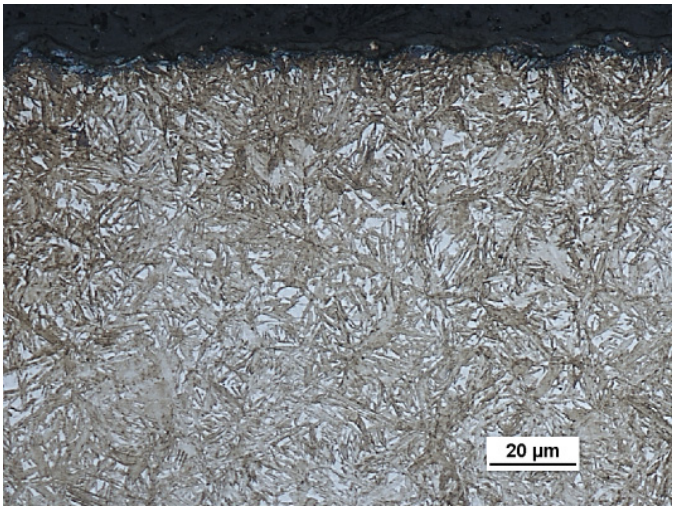

Fig. 2. Microstructure of the surface layer of AMS6265 steel after low pressure carburizing and gas quenching

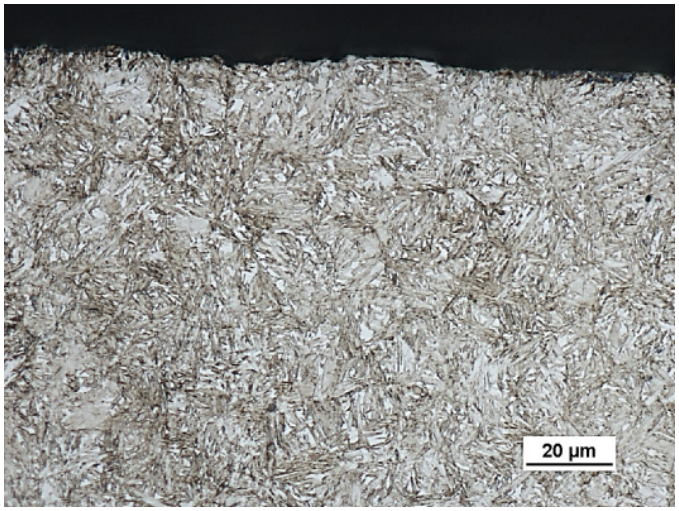

Fig. 3. Microstructure of the surface layer of AMS6265 steel after low pressure carburizing with oil hardening

Figure 5 shows the distribution of micro-hardness as a function of the distance from the surface for AMS6265 steel obtained by vacuum carburizing and gas- and oil-quenching. Hardness tests were made in accordance with standard PN-ISO 2639:2005, at load 10 N (HV1).

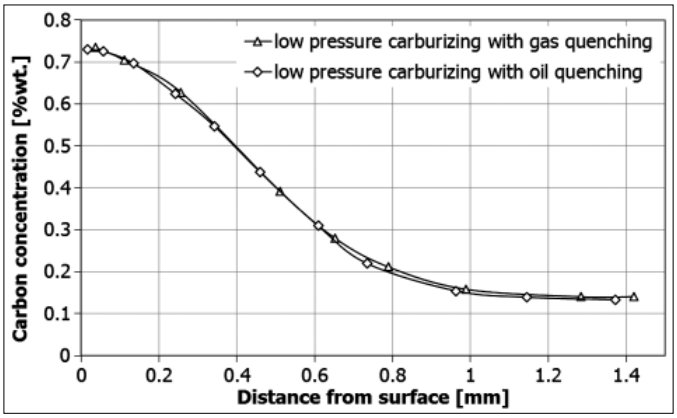

Fig. 4. The carbon profiles after low pressure carburizing processes of AMS6265 steel

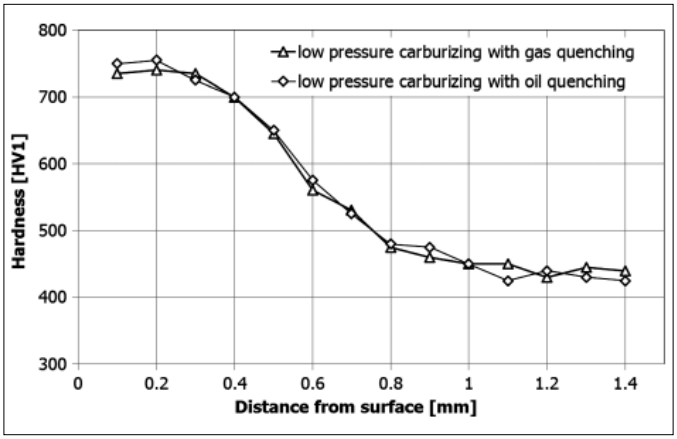

Fig. 5. Microhardness profiles of AMS6265 steel after low pressure carburizing with hardening

This was followed by determination of internal stresses in gear wheels subjected to two variants of thermal treatment. The measurements were conducted for the same teeth on each wheel, no. 1, 6, 12, 18 and 24 (Fig. 6). Stress measurements were conducted by the X-ray method $\sin^2\psi$ with use of the x-ray diffractometer, in accordance with standard SAE HS-784. Residual stresses distribution was measured by X-ray $\sin 2\psi$ diffraction method on PROTO iXRD analyzer. X-ray tube generating characteristic CrKα radiation was applied. Characteristic ferritic peak positions were measured at 2Θ angle equal 156° giving diffraction patterns from (211) planes. Measurements were performed for eleven (five positive, five negative and "0") Psi (ψ) angles in the range from + 30° to – 30° in relation to β angle. Diffraction peak positions were analyzed by Pearson VII peak fit function. Measurements were performed on the pitch diameter of examined teeth.

The geometry of the measurement is presented in Figure 7 [20].

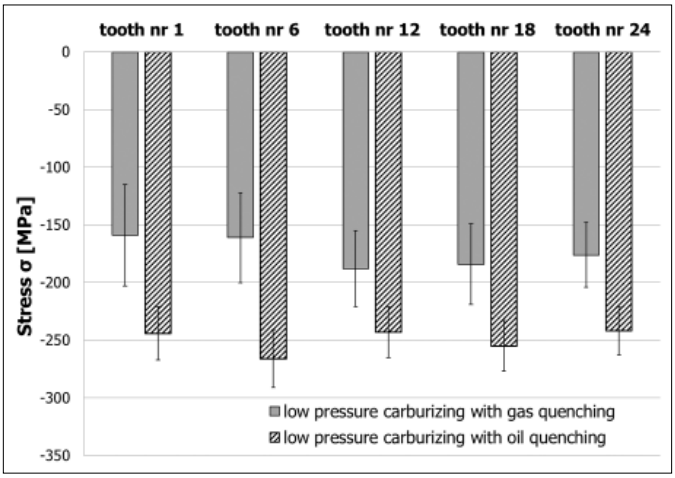

Fig. 6. Residual stresses in gear wheels made of AMS6265 steel after low pressure carburizing with hardening

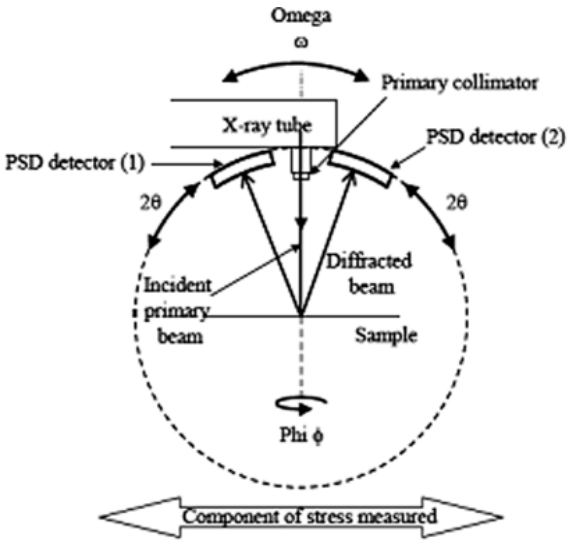

Fig. 7. The sin2ψ measurement geometry applied in investigations

Measurements of the gear wheels used in the experiment were performed in order to determine the effect of thermal treatment on deformations. Radial run-out was measured on the pitch diameter before and after carburizing with quenching. Radial run-out was measured with an accuracy of ±1 µm by gearwheel measurement device manufactured by Carl Zeiss Jena. The measurements were performed for each gear wheel by determination of the radius from the rotation axis to the pitch diameter. The measurement results are shown in the diagrams presented in Figures 8 and 9. The mean deformation is 6 ±4 µm after gas quenching and 12 ±9 µm after oil quenching. Next measurement was made of the tooth thickness of each of the gear wheels on three different heights: on the head tooth (h_1), on the pitch diameter (h_2) and on the foot of the tooth (h_3). The measuring position from the top of a tooth was: 1.5 mm (h_1), 5.0 mm (h_2) and 9.5 mm (h_3), as shown in Figure 10. The results of these study are presented in Figures 11 and 12. The average size of the deformation the thickness of the teeth for the gear wheels after gas – and oil – quenching presented in Table 2.

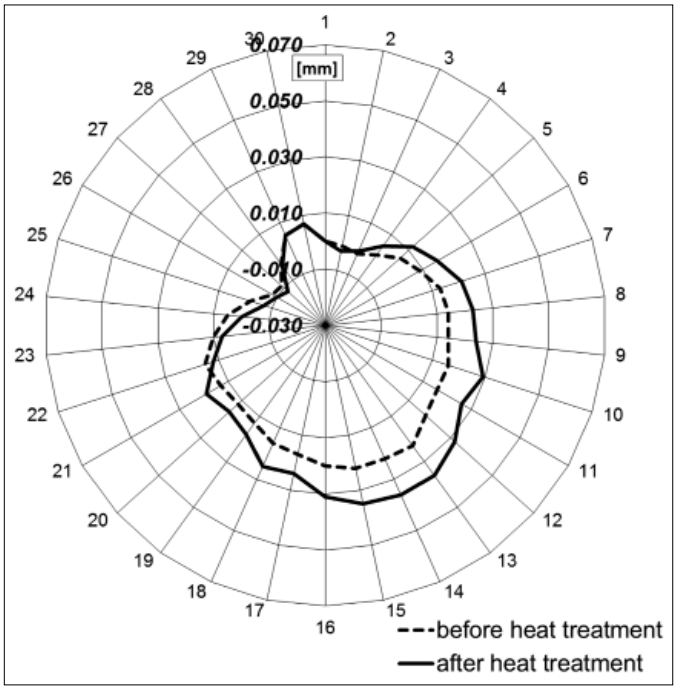

Fig. 8. Radial run-out of gear wheels made of AMS6265 steel before and after low pressure carburizing with gas hardening

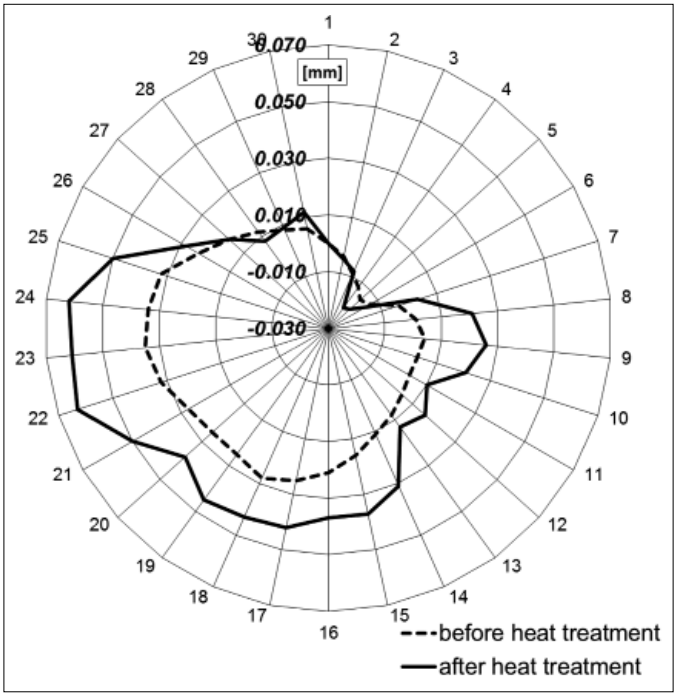

Fig. 9. Radial run-out of gear wheels made of AMS6265 steel before and after low pressure carburizing with oil hardening

TABLE 2

The average size of the deformation the thickness of the teeth for the gear wheels after gas- and oil-quenching

Quenching method	Tooth thickness [µm]		
	t_1	t_2	t_3
gas	9 ±6	27 ±8	31 ±3
oil	56 ±8	4 ±3	5 ±2

The treatment performed in this experiment resulted in the correct structure of the surface layer of AMS6265 steel, typical for carburized and quenched layer with the same phase composition, regardless of the method of quenching applied (Fig. 2, 3). Layers consistent with the design, with the specified carbon distribution of and hardness profile, were obtained in each of the treatment variants (Fig. 4, 5). Residual stresses in gear wheels after low pressure carburizing with gas quenching were about 100MPa lower than in gear wheels after oil hardening. The pitch diameter was found to increase around the whole perimeter of the gearwheel after the treatment. A comparison of the deformations for each gearwheel has shown that vacuum carburizing followed by high-pressure gas quenching resulted in lower deformations than vacuum carburizing followed by oil quenching (Fig. 8, 9). The average radial deformation was measured on the pitch diameter is about 50% lower, although higher the residual stresses after oil quenching. Unlike with oil quenching, the deformations formed with gas quenching are more uniform.

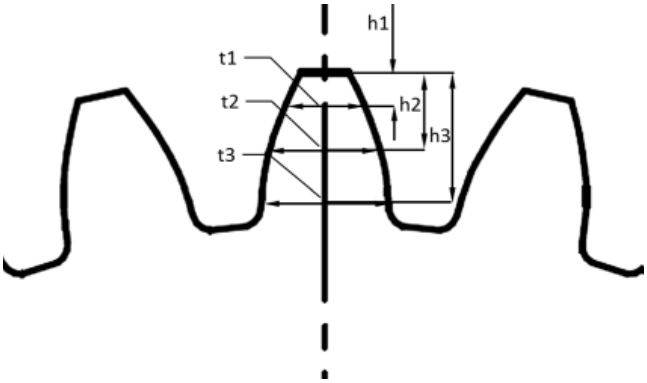

Fig. 10. Places of the thickness measurement of teeth

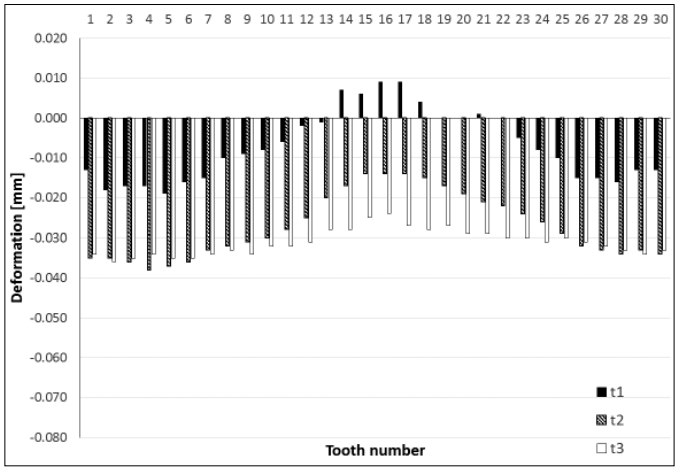

Fig. 11. Deformation of gear teeth made of AMS6265 steel after low pressure carburizing with gas hardening

Deformation of teeth formed after carburizing with gas hardening is characterized by high uniformity over the tooth (Fig. 11). After oil hardening the very high inhomogeneity of deformation was observed – huge on the head tooth, slightly on the pitch diameter and the rate of tooth (Fig. 12, Table 2).

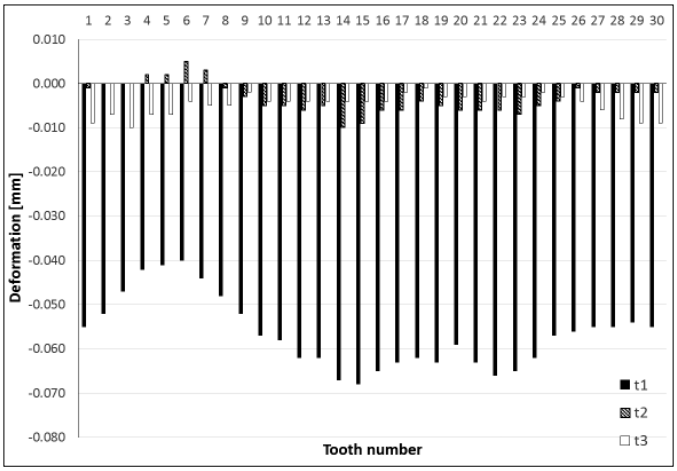

Fig. 12. Deformation of gear teeth made of AMS6265 steel after low pressure carburizing with oil hardening

Deformation of the head tooth is many times higher than the foot of the tooth. This is due to the difference in cooling rate between gas and oil . In the case of hardening in oil higher cooling rate resulted in an increase in deformation of the head tooth.

4. Conclusions

The following conclusions can be drawn from this experiment:

1. Compared to high-pressure gas quenching after vacuum carburizing, oil quenching resulted in the increase of deformations.
2. Unlike with oil quenching, deformations formed with gas quenching were more uniform, which helps to predict the deformation and the size of excess to correct the dimensions following heat treatment.
3. In the case of gear wheels made of steel of higher hardenability, cooling the gas after vacuum carburizing is better than oil quenching, taking into account the size and character of deformation.

Acknowledgements

This study was conducted within the project INNOTECH-K1/IN1/5/159396/NCBR/12

REFERENCES

[1] W. Gräfen, B. Edenhofer, Surf. Coat. Tech. **200**, 1830-1836 (2005).
[2] P. Kula, K. Dybowski, E. Wolowiec, R. Pietrasik, Vacuum. **99**, 175-179 (2014).
[3] W. Gräfen, M. Hornung, O. Irretier, M. Rink, Haerterei Tech. Mit. **62**(3), 97-102 (2007).
[4] P. Kula, Ł. Kaczmarek, K. Dybowski, R. Pietrasik, M. Krasowski, Vacuum. **87**, 26-29 (2013).

[5] D.H. Herring, R.L. Houghton, Proc. of the Sec. Intern. Conf. Carburizing and Nitriding with Atmospheres, Cleveland. 103-108 (1995).

[6] P. Kula, R. Pietrasik, K. Dybowski, S. Pawęta, E. Wołowiec, Adv. Mat. Res. 452-453, 401-406 (2012).

[7] P. Kula, E. Wołowiec, R. Pietrasik, K. Dybowski, B. Januszewicz, Vacuum. **88**, 1-7 (2013).

[8] J. Sawicki, M. Górecki, Ł. Kaczmarek, Z. Gawroński, K. Dybowski, R. Pietrasik, W. Pawlak, Chiang. Mai. J. Sci. **40**(5), 886-897 (2013).

[9] Z. Gawroński, A. Malasiński, J. Sawicki, Int. J. Automot. Techn. **11**(1), 127-131 (2012).

[10] F.T. Hoffmann, T. Lübben, P. Mayr, Heat. Treat. Met. **3**, 63-67 (1999).

[11] R. Atraszkiewicz, B. Januszewicz, Ł. Kaczmarek, W. Stachurski, K. Dybowski, A. Rzepkowski, Mat. Sci. Eng. A-Struct. **558**, 550-557 (2012).

[12] K. Loeser, V. Heuer, D.R. Faron, HTM Härterei- Technische Mitteilungen. **61**(6), 326-329 (2006).

[13] P. Jurči, P.Stolař, BHM Berg- und Hüttenmännische Monatshefte. **151**(11), 437-441 (2006).

[14] F. Preisser, G. Seemann, W.R .Zenker, Proc. of the 1st International Automotive Heat Treating Conference, Puerto Vallarta, Mexico. 135-147 (1998).

[15] J. Cieślik, P. Kula, S. Filipek, J. Alloy. Compd. **480**, 612-616 (2009).

[16] J. Sawicki, A. Gutkowski, I. Kaczmarek, S. Paweta, A. Rylski, Met. Sci. Heat Treat. **56**(11-12), 685-689 (2015).

[17] European Patent No.: EP1558780 (2007), United States Patent No.: US 7513958 (2009).

[18] SAE HS-784 – Residual Stress Measurement by X-Ray Diffraction, 2003 Edition.

[19] ASTM E-975 – Standard Practice for X-Ray Determination of Retained Austenite in Steel with Near Random Crystallographic Orientation.

[20] M.E. Fitzpatrick, A.T. Fry, P. Holdway, F.A. Kandil, J. Shackleton, L. Suominen, Determination of residual stresses by X-Ray diffraction, Measurement Good Practice Guide No. 52, National Physical Laboratory, Teddington, UK (2005).